CONDENSATION OF SUPERSATURATED VAPOURS. HOMOGENEOUS NUCLEATION OF NAPHTHALENE AND PHTHALIC ANHYDRIDE

Jiří Smolík and Jaroslav Vítovec

Institute of Chemical Process Fundamentals, Czechoslovak Academy of Sciences, 165 02 Prague 6 - Suchdol

Received October 18th, 1984

The critical supersaturation required for the homogeneous nucleation of naphthalene and phthalic anhydride from their vapours has been measured using upward thermal diffusion cloud chamber. The results obtained are compared with the predictions of the classical theory of homogeneous nucleation (Volmer–Becker–Döring–Zeldovich) and the corresponding states correlation of homogeneous nucleation. The classical theory is found to be in excellent agreement with the experimental results on naphthalene but overpredicts the critical supersaturation of phthalic anhydride vapours by about 30%. In order to fit the experiment and theory, the new values of surface tension of phthalic anhydride were recalculated from the theory. Critical supersaturation of naphthalene plotted versus temperature reveals the same regular departure from single fluid behaviour as found for alkylbenzenes. The experimental results on phthalic anhydride were found to be in very good agreement with the corresponding states correlation.

It has long been known that nonisothermal diffusion can produce supersaturation of vapour phase in the vicinity of evaporating or condensing surfaces. If the vapour phase contains foreign particles, ions, or sufficiently large clusters of its own molecules, extremely rapid condensation will occur on these nuclei to form dispersion of droplets or crystallites. Such nucleation-condensation phenomena usually lead to complications in the operation of an apparatus. For example in boundary-layer condensation over hot surface, the precipitate is a sink for vapour, so its formation steepens the pressure gradient and accelerates mass transfer. In the case of cooler--condenser the precipitation is often associated with loss of the material in the condenser effluent and results in air pollution. Thus understanding of nucleation phenomena can be useful in designing vaporisation-condensation processes.

When foreign particles are present and the supersaturation is low, condensation takes place on the existing particles. At sufficiently high supersaturation, the rate of self-nucleation (homogeneous nucleation) increases rapidly and high concentrations of very small particles are generated. The rate of homogeneous nucleation varies sharply with supersaturation. It is negligible below some characteristic value of supersaturation and increases dramatically above it. This characteristic value is designated as the critical supersaturation S_{crit}, defined as the ratio of the actual

pressure to the equilibrium vapour pressure at the temperature in question, and is related usually to the rate of nucleation $J = 1$ particle $cm^{-3} s^{-1}$. Thus S_{crit} represents a very useful criterion for "misting" in the supersaturated vapour. As mentioned before "misting" can occur at condensation of hot vapour-gas mixtures. Two such examples are isolation of phthalic anhydride from hot vapour–air mixture in the „switch condenser" or desublimation of naphthalene from vapour-gas mixtures in the transpiration crystallizer. The aim of this paper was therefore to determine experimentally the critical supersaturation S_{crit} for both these compounds. Experiments were carried out by using an upward thermal diffusion cloud chamber.

EXPERIMENTAL

Apparatus. In the upward thermal diffusion cloud chamber vapour is supersaturated at nonisothermal flow of substance evaporated from the pool of liquid on hot bottom plate and condensing on cooled top plate of the chamber. The onset of homogeneous nucleation is determined visually by observing the forward scattering of light from drops formed by the nucleation process. The chamber used here is similar to the chamber described in previous studies[1,2]. Only details unique to the present study are mentioned. The top and bottom plates are duralumin alloy discs, 25 mm thick and 200 mm o.d.. The top plate is machined to have 1° bevel to allow the condensate to drain off to the sides of the chamber. Two holes are drilled through this plate to allow filling of the chamber with inert gas and adjustment of the pressure. The temperature of top plate near the condensing surface was measured by calibrated NiCr–Ni thermocouple. This thermocouple was placed in a well drilled to 0·5 mm of the lower surface. The temperature of the surface of the liquid pool on the bottom plate was measured by two calibrated NiCr–Ni thermocouples, 0·15 mm in diameter. The thermocouples were brought into the chamber through this plate at a point just inside the inner wall and led radially into the centre of the plate. The chamber wall was 26 mm high glass ring, 165 mm i.d. (diameter to height ratio 6·3 : 1), heated by a resistance wire wrapped around. The chamber was sealed by silicon rubber gaskets in the case of phthalic anhydride and Viton gaskets in the case of naphthalene.

Compounds. Naphthalene and phthalic anhydride (both pure grade, Lachema, Brno) were zonally refined. Helium (Messe Griesheim GmbH., Austria) with purity 99·996% was supplied from a pressure cylinder.

RESULTS

Critical supersaturation of vapours of naphthalene was measured within the range of temperatures 350–410 K and of vapours of phthalic anhydride within the range of 390–450 K. The upper limit for naphthalene was given by low pressure ratio effect[3]. As found experimentally[3–6], the observed critical supersaturations are independent of the amount of carrier gas as long as the ratio of total pressure to the equilibrium pressure of the substance being measured at the temperature of the hot plate is greater than about 2. Thus for higher temperatures higher pressure of the carrier gas must be used and experiments are then limited for danger of rupturing

of the glass ring. The upper limit for phthalic anhydride experiments was given by decomposition of this compound at higher temperatures. In these experiments, the brownish spot of the products of decomposition appeared in the pool of phthalic anhydride and the yellowish spot of some more volatile product was found on the corresponding place of condensate after solidifying. It was observed simultaneously that the light with the wavelengths shorter then 430 nm caused an increase in the nucleation rate in the corresponding volume of the chamber. It corresponds well to the yellowish colour of the volatile products. The observed effect thus can be explained by a nucleation induced by photoexcited molecules[7] of volatile products of decomposition. To avoid it the fresh phthalic anhydride was used in the individual experiments and a yellow filter was used for illumination. The lower limits of temperature range for both compounds were given by degree of supercooling of condensate on the upper plate. While for naphthalene the supercooling of 7 K below normal freezing point was achieved at steady-state operating conditions, in the case of phthalic anhydride the progressive cooling of the upper plate had to be used. The parameters characterising the state of the chamber and corresponding in the individual experiments to the observed rate of condensation $J \approx 1$ drop $cm^{-3}\ s^{-1}$ are listed in Table I.

The parameters, given in Table I, were used for calculation of supersaturation in each experiment. It consists of solution of a set of ordinary nonlinear differential equations for the steady-state and a set of nonlinear partial differential equations for the nonsteady-state operating conditions[2,8]. Physical properties of individual compounds, necessary for experimental data evaluation are listed in the Appendix. They were taken predominantly from the literature or fitted to the available experimental data. When data for these properties were unavailable they were estimated by reliable theoretical or empirical methods. However, using different formulas considerably different values of physical properties were obtained. Thus for example, the comparison of recently published data on diffusion coefficient of naphthalene in hydrogen[9] (*i.e.* similar to our system) with calculated values gives the deviation 5·5% for usually applied Gidding's semiempirical correlation[10] and the deviation −12% for the Chapman–Enskog kinetic theory[11]. Similarly, the thermal diffusion factors calculated from the first Kihara approximation to the Chapman–Enskog theory[12] were substantially higher (and in the case of naphthalene–He mixture close to experimental data[13]) than usual accepted approximation $\alpha = 0{\cdot}3$.

It has already been shown that the error inherent in estimation methods has an insignificant effect on the supersaturation profile in the chamber[3–5]. However, relatively small changes in thermal diffusion factor were assumed. The calculation based on kinetic theory and also some experimental results[13] indicate that substantially higher values of thermal diffusion factor should be used. It caused for example an 30% increase in supersaturation profiles in stearic acid experiments[2]. To verify it we solved heat and mass flux equations for each experiment with *a*) all properties

calculated using Chapman–Enskog kinetic theory and *b*) diffusion coefficient calculated using Gidding's semiempirical correlation and $\alpha = 0{\cdot}3$.

In Figs 1 and 2 the portions of supersaturation profiles near the peak are shown *versus* the corresponding temperatures for naphthalene and phthalic anhydride, respectively. The individual experiments were evaluated with physical properties

TABLE I

Experimental data: T_1 the temperature of the pool surface, T_2 the temperature at the surface of the liquid film condensed on the top plate or its initial value, T_3 the final temperature of the liquid film surface, r the rate of the cooling of the top plate and P_t the total pressure in the chamber. Stability criterion: P_t/P_1, the pressure ratio. P_1 is the equilibrium vapour pressure of the working fluid at T_1

Experiment	T_1, K	T_2, K[a]	T_3, K[a]	r, K min^{-1}	P_t, kPa	P_t/P_1
			Naphthalene			
1	457·0	347·9	—	—	134·653	3·10
2	466·2	352·2	—	—	145·719	2·64
3	458·4	349·3	—	—	148·385	3·30
4	461·1	351·0	—	—	150·385	3·11
5	465·7	353·7	—	—	153·718	2·82
6	472·6	354·6	—	—	133·784	2·06
7	471·2	356·4	—	—	149·718	2·39
8	478·2	360·1	—	—	156·384	2·10
9	483·9	363·7	—	—	165·183	1·94
10	485·7	365·5	—	—	175·315	1·97
11	488·9	365·6	—	—	167·317	1·75
12	504·0	372·9	—	—	200·380	1·49
			Phthalic Anhydride			
1	496·3	413·8	392·0	3·03	104·523	4·22
2	492·2	409·5	390·9	2·77	103·323	4·61
3	498·4	411·5	395·6	2·15	127·187	4·98
4	504·2	412·0	399·2	2·03	129·987	4·29
5	507·1	408·2	402·9	1·54	130·654	4·03
6	505·4	403·1	—	—	112·522	3·63
7	505·9	404·2	—	—	112·522	3·58
8	515·1	406·6	—	—	116·656	2·95
9	513·2	406·8	—	—	116·788	3·09

[a] The temperatures of film surface T_2 and T_3 are the temperatures of the upper plate corrected for liquid film thickness[6].

calculated using kinetic theory of gases. The envelope to the individual curves (in Figs 1 and 2 denoted by dashed line) represents the experimental critical supersaturation curve. It was approximated by an empirical fitting formula

$$\ln S_{\text{crit.}} = (A + B/T)^{1.5} . \qquad (1)$$

To determine parameters A and B the method of least squares was used. Both parameters were chosen to minimize the sum of the squares of the distances of the points on the individual supersaturation curves and on the envelope having the same derivative. For both compounds, we fitted supersaturation *versus* temperature curves calculated using both sets of diffusion coefficient and thermal diffusion factors. The parameters of fitting formula (*1*) are presented in Table II.

The calculated experimental critical supersaturation curves are compared in Fig. 3 for naphthalene and in Fig. 4 for phthalic anhydride. Maximal percentage error caused by using different parameters at evaluation was found to be 1·9% for naphthalene and 5·7% for phthalic anhydride (in Figs 3 and 4 curves *1* and *2*). These

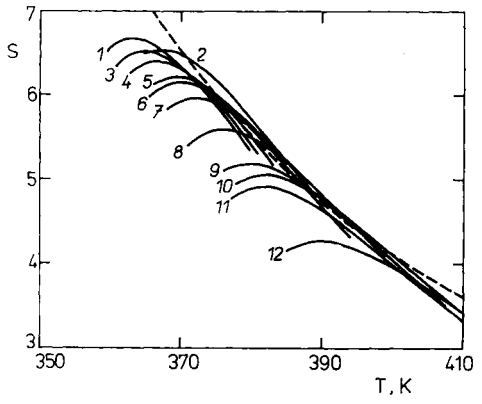

FIG. 1

Variation of the critical supersaturation of naphthalene vapour as a function of temperature. The numbered curves are the solutions of the transport equations for each experiment (Table I) obtained using diffusion coefficient and thermal diffusion factor calculated from kinetic theory of gases. The dashed line, which represents the envelope of the numbered curves, is the experimental result

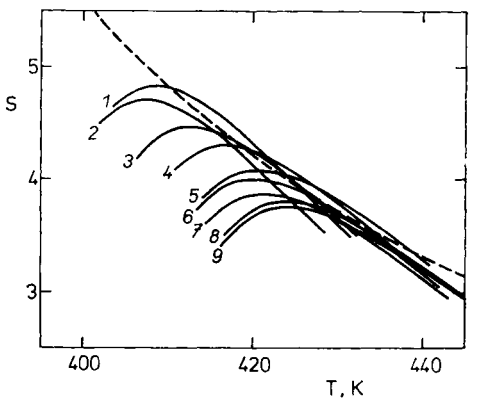

FIG. 2

Variation of the critical supersaturation of phthalic anhydride vapour as a function of temperature. The meaning of the curves as in Fig. 1

differences are comparable with usually accepted 5% uncertainty inherent to cloud chamber measurement. This confirms the statement that if most of the properties used in the heat and mass flux equation are unavailable in the literature, the supersaturation profiles can be accurately determined from estimated properties[5]. Also plotted on both figures are the predictions by the classical (Volmer–Becker–Döring–Zeldovich) theory[14] of homogeneous nucleation of supersaturation which will cause a rate of nucleation of 1 nuclei $cm^{-3}\ s^{-1}$ (lower dashed curve) and 100 nuclei $cm^{-3}\ s^{-1}$ (upper dashed curve). In the case of naphthalene, the agreement of experiment with the prediction of the classical theory is very good. For phthalic anhydride, the difference between experiment and theory is about 30% in the whole

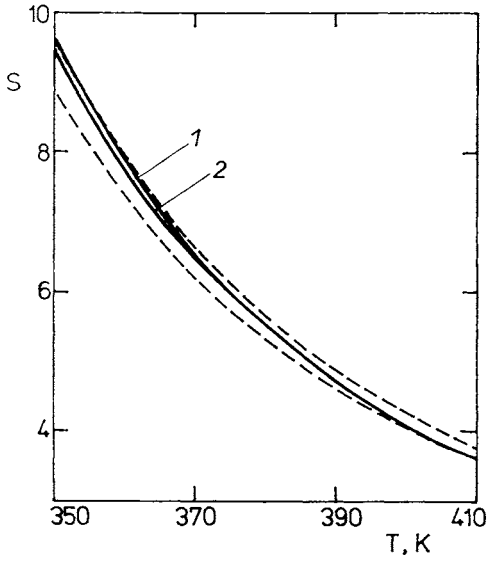

FIG. 3

Comparison theory and experiment for naphthalene. The solid lines are the experimental critical supersaturations of naphthalene vapours obtained using both diffusion coefficient and thermal diffusion factor calculated from the kinetic theory of gases (line *1*) and diffusion coefficient calculated using Gidding's semiempirical correlation and thermal diffusion factor $\alpha = 0{\cdot}3$ (line 2). The classical theory of homogeneous nucleation for rates of nucleation of 1 and 100 nuclei $cm^{-3} . s^{-1}$ is represented by lower and upper dashed curves, respectively

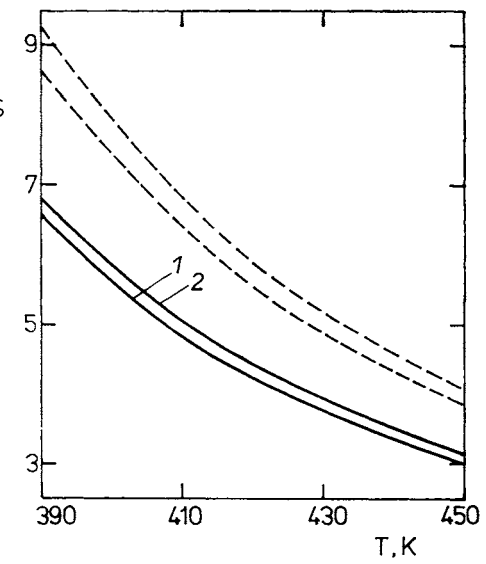

FIG. 4

Comparison theory and experiment for phthalic anhydride. The meaning of the curves as in Fig. 3

range of temperatures. This discrepancy might be caused by uncertainty of physical parameters used to calculate the theoretical variation of supersaturation with temperature. From these parameters, the accuracy of the values of the surface tension is critical since the rate of nucleation predicted by theory is strongly dependent

TABLE II

Parameters of fitting formula (*1*). The data for each experiment were evaluated using (*a*) diffusion coefficient and thermal diffusion factor calculated using Chapman–Enskog kinetic theory and (*b*) diffusion coefficient calculated using Gidding's semiempirical correlation and thermal diffusion factor $\alpha = 0{\cdot}3$

Method	*A*	*B*
	Naphthalene	
a	−1·9934	1 301·4
b	−1·9544	1 284·7
	Phthalic anhydride	
a	−1·9466	1 353·8
b	−1·7846	1 297·3

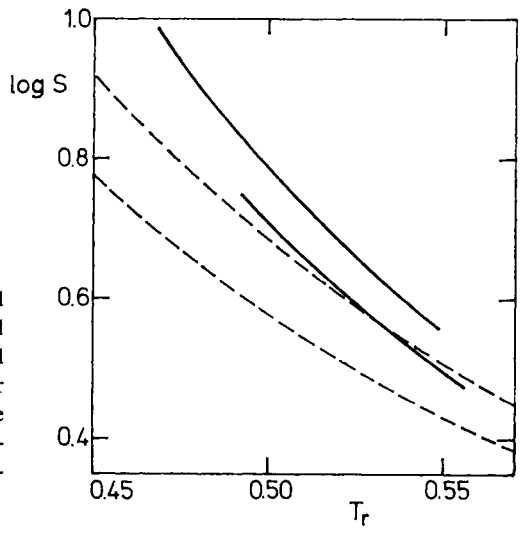

FIG. 5

Critical supersaturation ratio *vs* reduced temperature; the solid lines are experimental critical supersaturations of naphthalene and phthalic anhydride vapours (upper and lower line, respectively). The dashed lines are corresponding states correlation of the homogeneous nucleation of supersaturated vapours[17]

on surface tension. The variation of the surface tension of liquid phthalic anhydride with temperature was obtained only from the two values, without specification of their origin[15] (experimental or calculated). The fact that they could be perfectly correlated with experimental densities[16] using MacLeod–Sugden correlation[11] (with value of parachor $[P] = 301$ slightly higher than our calculation $[P] = 291{\cdot}4$) indicates that both values were probably calculated. Thus, the surface tension required to fit theoretical and experimental critical supersaturation was calculated and following relation was obtained

$$\sigma = 85{\cdot}3 - 0{\cdot}125T, \quad \text{mN/m} \quad (390-450\ \text{K}). \tag{2}$$

It represents variation of surface tension of liquid phthalic anhydride with temperature experimentally determined *via* supersaturation measurements.

In Fig. 5, the experimental results are compared with McGraw's[17] corresponding states correlation of the homogeneous nucleation of supersaturated vapour (represented by the dashed curve boundaries, see ref.[17]). While the results on naphthalene reveal the same regular departure from simple fluid behaviour like alkylbenzenes[17] more interesting is the very good agreement for nonspherical and strongly polar substance phthalic anhydride.

APPENDIX

Physical properties of naphthalene were taken from the book by Yaws[18], force constants were calculated using critical properties[11]. Physical properties of phthalic anhydride were taken predominantly from the Physical Property Data Bank of Reid and coworkers[11] and monography by Suter[16]. Vapour pressure data[19–21] from the interval 387–558 K were fitted to the Antoine form by the method of nonlinear least squares. The temperature dependence of surface tension was fitted to the literature data[15]. Pitzer accentric factor was calculated using critical properties, force constants were calculated using Brokaw's correlation for polar gases[11]. For estimation of viscosity and thermal conductivity of vapour phthalic anhydride the Chapman–Enskog kinetic theory was used[11]. Thermal conductivity of liquid phthalic anhydride was estimated by the method of Sato and Riedel[11]. For the temperature dependence of enthalpy of vaporization, the Watson correlation[11] was used. The binary diffusion coefficients for both systems were calculated using kinetic theory[11] or Gidding's semiempirical correlation[10]. Thermal diffusion factors were estimated from the first Kihara approximation to the Chapman–Enskog theory[12]. The calculated values were correlated by the equation suggested by Kokugan and Shimizu[22]. The parameters of dependence of thermal conductivity on composition were estimated by Lindsay–Bromley method[11].

The values of the parameters actually used are listed below. Subscripts g and l denote property in the gaseous or liquid state, symbols have the following meaning: T temperature, P pressure, ω Pitzer accentric factor, σ and ε/k force constants, c specific heat, λ thermal conductivity, μ viscosity, ϱ density, σ surface tension, ΔH enthalpy of vaporization, V_b molar volume of the liquid at the normal boiling point T_b, p dipole moment, D_{12} binary diffusion coefficient, A_{12}, A_{21} Lindsay-Bromley parameters, α thermal diffusion factor, R gas constant and x mole fraction.

Naphthalene

$T_b = 491{\cdot}1$ (K)
$T_c = 748{\cdot}2$ (K)
$P_c = 4{\cdot}011$ (MPa)
$\omega = 0{\cdot}295$
$\sigma = 6{\cdot}204 \cdot 10^{-10}$ (m)
$\varepsilon/k = 629{\cdot}55$ (K)
$c_{p,g} = -54{\cdot}51 + 0{\cdot}7746T - 5{\cdot}275 \cdot 10^{-4}T^2 + 1{\cdot}336 \cdot 10^{-7}T^3$ (J/K mol)
$c_{v,g} = -0{\cdot}49 + 6{\cdot}033 \cdot 10^{-3}T - 4{\cdot}116 \cdot 10^{-6}T^2 + 1{\cdot}042 \cdot 10^{-9}T^3$ (J/K g)
$\lambda_g = -9{\cdot}378 + 4{\cdot}936 \cdot 10^{-2}T + 3{\cdot}81 \cdot 10^{-5}T - 1{\cdot}063 \cdot 10^{-8}T^3$ (mW/m K)
$\lambda_l = 132{\cdot}82 + 5{\cdot}954 \cdot 10^{-2}T - 1{\cdot}69 \cdot 10^{-4}T^2$ (mW/m K)
$\mu_g = -2{\cdot}486 + 2{\cdot}765 \cdot 10^{-2}T - 4{\cdot}955 \cdot 10^{-6}T^2$ (μPa s)
$\log \mu_l = -4{\cdot}46 + 1\,093/T + 0{\cdot}4767 \cdot 10^{-2}T - 2{\cdot}548 \cdot 10^{-6}T$ (mPa s)
$\varrho_l = 324{\cdot}1 - 0{\cdot}2653^{-(1-T_r)^{2/7}}$ (kg/m^3)
$\sigma = 81{\cdot}0(1 - T_r)^{1.3511}$ (mN/m)
$\log P_{eq.} = 194{\cdot}285 - 8336{\cdot}3/T - 72{\cdot}834 \log T + 56{\cdot}768 \cdot 10^{-3}T - 17{\cdot}319 \cdot 10^{-6}T^2$ (Pa)
$\Delta H_{ev.} = 43\,305{\cdot}4((1 - T_r)/(1 - T_{br}))^{0.38}$ (J/mol)

Phthalic anhydride

$T_b = 557{\cdot}4$ (K)
$T_c = 810$ (K)
$P_c = 4{\cdot}762$ (MPa)
$V_b = 128{\cdot}9$ (cm^3/mol)
$p = 17{\cdot}39 \cdot 10^{-30}$ (C . m)
$\omega = 0{\cdot}6$
$\sigma = 5{\cdot}13 \cdot 10^{-10}$ (m)
$\varepsilon/k = 1\,080$ (K)
$c_{p,g} = -4{\cdot}4548 + 0{\cdot}65398 \cdot T - 4{\cdot}2831 \cdot 10^{-3}T^2 + 1{\cdot}0094 \cdot 10^{-6}T^3$ (J/K . mol)
$c_{v,g} = -0{\cdot}086213 + 4{\cdot}4153 \cdot 10^{-3}T - 2{\cdot}8917 \cdot 10^{-6}T^2 + 6{\cdot}815 \cdot 10^{-10}T^3$ (J/K . g)
$\lambda_g = -6{\cdot}916 + 5{\cdot}0658 \cdot 10^{-5}T$ (mW/m . K)
$\lambda_l = 0{\cdot}1823 - 1{\cdot}63 \cdot 10^{-4}T$ (W/m . K)
$\mu_g = 0{\cdot}854 + 2{\cdot}151 \cdot 10^{-2}T$ (μPa . s)
$\mu_l = 1{\cdot}7869 \exp(1\,702{\cdot}37/T)$ (μPa . s)
$\varrho_l = 1\,623{\cdot}3 - 0{\cdot}985T$ (kg/m^3)
$\sigma = 83{\cdot}3 - 0{\cdot}1116T$ (mN/m)
$\log P_{eq.} = 8{\cdot}43034 - 1\,385{\cdot}77/(T - 153{\cdot}58)$ (Pa)
$\Delta H_{ev.} = 65\,419{\cdot}0((1 - T_r)/(1 - T_{br}))^{0.38}$ (J/mol)

Helium

$\sigma = 2{\cdot}551 \cdot 10^{-10}$ (m)
$\varepsilon/k = 10{\cdot}22$ (K)
$c_{c,g} = 20{\cdot}79$ (J/K . mol)
$c_{v,g} = 3{\cdot}118$ (J/K . g)
$\lambda_g = 3{\cdot}72 \cdot 10^{-2} + 3{\cdot}91 \cdot 10^{-4}T - 7{\cdot}49 \cdot 10^{-8}T^2 + 1{\cdot}29 \cdot 10^{-11}T^3$ (W/m . K)
$\mu_g = 1{\cdot}4808T^{1{\cdot}5}/(T + 87{\cdot}609)$ (μPa . s)

Naphthalene(1)–helium(2)

$$D_{12} = 1{\cdot}4241 \cdot 10^{-5} RT^{1{\cdot}75}/P \quad (m^2/s), \quad P(Pa), \text{ ref.}^{10}$$
$$D_{12} = 1{\cdot}94 \cdot 10^{-5} RT^{1{\cdot}7163}/P \quad (m^2/s), \quad P(Pa), \text{ ref.}^{11}$$
$$A_{12} = 0{\cdot}21, \quad A_{21} = 9{\cdot}4 \quad \lambda_{12} = \frac{\lambda_1 x_1}{x_1 + A_{12} x_2} + \frac{\lambda_2 x_2}{x_2 + A_{21} x_1}$$
$$1/\alpha = (-0{\cdot}854 + T/(0{\cdot}2874T + 23{\cdot}94)) \cdot (x_1 + 0{\cdot}124) + 0{\cdot}105$$

Phthalic anhydride(1)–helium(2)

$$D_{12} = 1{\cdot}556 \cdot 10^{-5} RT^{1{\cdot}75}/P \quad (m^2/s), \quad P(Pa), \text{ ref.}^{10}$$
$$D_{12} = 1{\cdot}785 \cdot 10^{-5} RT^{1{\cdot}7657}/P \quad (m^2/s), \quad P(Pa), \text{ ref.}^{11}$$
$$A_{12} = 0{\cdot}22, \quad A_{21} = 8{\cdot}7$$
$$1/\alpha = (-0{\cdot}804 + T/(0{\cdot}3055T - 35{\cdot}58)) \cdot (x_1 + 0{\cdot}161) + 0{\cdot}129$$

REFERENCES

1. Smolík J., Vítovec J.: J. Aerosol Sci. *13(6)*, 587 (1982).
2. Smolík J., Vítovec J.: J. Aerosol Sci. *14(6)*, 697 (1983).
3. Katz J. L., Scoppa II C. J., Canesh Kumar N., Mirabel P.: J. Chem. Phys. *62*, 448 (1975).
4. Katz J. L., Mirabel P., Scoppa II C. J., Virkler T. L.: J. Chem. Phys. *65*, 382 (1976).
5. Becker C., Reiss H., Heist R. H.: J. Chem. Phys. *68*, 3585 (1978).
6. Katz J. L.: J. Chem. Phys. *52*, 4733 (1970).
7. Katz J. L., Wen F. C., McLaughlin T., Rausch R. J., Partch J.: Science *196*, 1203 (1977).
8. Smolík J., Vítovec J.: Int. J. Heat Mass Transfer *26*, 975 (1982).
9. Caldwell L.: J. Chem. Eng. Data *29*, 60 (1984).
10. Fuller E. N., Ensley K., Giddings J. C.: J. Phys. Chem. *73*, 3697 (1969).
11. Reid R. C., Prausnitz J. M., Sherwood T. K.: *The Properties of Gases and Liquids*, 3rd Ed. McGraw-Hill, New York 1977.
12. Hirschfelder J. O., Curtiss C. F., Bird R. B.: *Molecular Theory of Gases and Liquids*. Willey, New York 1954.
13. Mazurenko Yu. T.: Zh. Fiz. Chim. *42*, 2193 (1968).
14. Abraham F. F.: *Homogeneous Nucleation Theory, The Pretransition Theory of Vapor Condensation*, Advances Teor. Chem. Suppl. 1. Academic Press, New York 1974.
15. *Kirk–Othmer Encyclopedia of Chemical Technology*, Vol. 15, p. 445. Willey, New York.
16. Suter H.: *Phthalsäureanhydrid und seine Verwendung*. D. Steinkopf Verlag, Darmstadt 1972.
17. McGraw R.: J. Chem. Phys. *75*, 5514 (1981).
18. Yaws C. L.: *Physical Properties, A Guide to the Physical, Thermodynamics and Transport Property Data of Industrially Important Chemical Compound*. Chemical Engineering, McGraw-Hill, New York 1977.
19. Monroe K. P.: Ind. Eng. Chem. *12*, 969 (1920).
20. Ramsay W., Young S.: Trans. Roy. Soc. London, *I. 1886*, 102, from ref.[19].
21. Crooks D. A., Feetham F. M.: J. Chem. Soc. *1946*, 899.
22. Kokugan T., Shimizu M.: J. Chem. Eng. Jap. *14*, 7 (1981).

Translated by the author (J. S.).